



Original contribution

Assessment of the patellofemoral cartilage: Correlation of knee pain score with magnetic resonance cartilage grading and magnetization transfer ratio asymmetry of glycosaminoglycan chemical exchange saturation transfer

Young Han Lee ^a, Jaemoon Yang ^a, Ha-Kyu Jeong ^b, Jin-Suck Suh ^{a,*}

^a Department of Radiology, Research Institute of Radiological Science, Medical Convergence Research Institute, and Severance Biomedical Science Institute, Yonsei University College of Medicine, Seoul, Republic of Korea

^b Clinical Science, Philips Healthcare, Seoul, Republic of Korea

ARTICLE INFO

Article history:

Received 26 May 2016

Revised 25 July 2016

Accepted 20 August 2016

Keywords:

Cartilage

Magnetic resonance imaging (MRI)

Chemical exchange saturation transfer

Magnetization transfer contrast imaging

ABSTRACT

Purpose: Biochemical imaging of glycosaminoglycan chemical exchange saturation transfer (gagCEST) could predict the depletion of glycosaminoglycans (GAG) in early osteoarthritis. The purpose of this study was to evaluate the relationship between the magnetization transfer ratio asymmetry (MTR_{asym}) of gagCEST images and visual analog scale (VAS) pain scores in the knee joint.

Materials and methods: This retrospective study was approved by the institutional review board. A phantom study was performed using hyaluronic acid to validate the MTR_{asym} values of gagCEST images. Knee magnetic resonance (MR) images of 22 patients (male, 9; female, 13; mean age, 50.3 years; age range; 25–79 years) with knee pain were included in this study. The MR imaging (MRI) protocol involved standard knee MRI as well as gagCEST imaging, which allowed region-of-interest analyses of the patellar facet and femoral trochlea. The MTR_{asym} at 1.0 ppm was calculated at each region. The cartilages of the patellar facets and femoral trochlea were graded according to the Outerbridge classification system. Data regarding the VAS scores of knee pain were collected from the electronic medical records of the patients. Statistical analysis was performed using Spearman's correlation.

Results: The results of the phantom study revealed excellent correlation between the MTR_{asym} values and the concentration of GAGs ($r = 0.961$; $p = 0.003$). The cartilage grades on the MR images showed significant negative correlation with the MTR_{asym} values in the patellar facet and femoral trochlea ($r = -0.460$; $p = 0.031$ and $r = -0.543$; $p = 0.009$, respectively). The VAS pain scores showed significant negative correlation with the MTR_{asym} values in the patellar facet and femoral trochlea ($r = -0.435$; $p = 0.043$ and $r = -0.671$; $p = 0.001$, respectively).

Conclusion: The pain scores were associated with the morphological and biochemical changes in articular cartilages visualized on knee MR images. The biochemical changes, visualized in terms of the MTR_{asym} values of the gagCEST images, exhibited greater correlation with the pain scores than the morphological changes visualized on conventional MR images; these results provide evidence supporting the theory regarding the association of patellofemoral osteoarthritis with knee pain scores.

© 2016 Elsevier Inc. All rights reserved.

1. Introduction

Joint pain in osteoarthritis (OA) is one of the most serious problems [1], along with synovial inflammation and progression of the cartilage lesions [2]. The patellofemoral joint (PFJ) is known to be

an important source of the symptoms associated with OA of the knee, and is possibly more important than the tibiofemoral joint (TFJ) [3]. Patellofemoral arthritis results from cartilage loss in the patella and trochlear groove. Cartilage loss can be assessed morphologically based on the radiography, computed tomography (CT), and magnetic resonance imaging (MRI) findings [4]. A previous study involving the evaluation of the difficulty levels of activities of daily living (ADL) reported no correlation between the ADL scores and the severity of patellofemoral arthritis assessed by radiography [5]. Moreover, a previous study on patellar cartilage stress had reported no significant differences in patellar cartilage stress

* Corresponding author at: Department of Radiology, Research Institute of Radiological Science, Medical Convergence Research Institute, and Severance Biomedical Science Institute, Yonsei University College of Medicine, 50-1 Yonsei-ro, Seodaemun-gu, Seoul, 03722, Republic of Korea. Tel.: +82 2 2228 7400; fax: +82 2 393 3035.

E-mail address: jss@yuhs.ac (J.-S. Suh).

between patients with PFJ pain and pain-free control subjects [6]. However, other biological factors might be involved in this complex pathway of pain.

Magnetic resonance imaging allows the direct visualization of articular cartilage. It enables qualitative and quantitative morphological assessment as well as characterization and quantification of the biochemical composition of the cartilage. Although PFJ pain is a multifactorial problem, increase in the T2 relaxation times of the patellar cartilage in a previous study was suggested as indicating early stages of patellar cartilage degeneration [7]. Several MRI techniques have been introduced for the quantitative imaging of cartilage, including the T1 ρ and T2 relaxation time mappings as well as the magnetization transfer ratio (MTR) mappings. Because of its relatively simple application in imaging, T2 relaxometry has been used for investigating the water and collagen content of cartilage [8–10]. Quantitative analysis using T2 relaxation time map has been shown to demonstrate increased values of the T2 constant at the medial patellar facet in patients with patellar friction syndrome, which could indicate early cartilage changes as well as increased water content [11]. Variations in T2 relaxation times are known to indicate early biochemical changes in cartilage degeneration prior to morphological changes [12–14]. As an alternative to the evaluation of water content in cartilage, the concentration of glycosaminoglycans (GAGs) in cartilage can be evaluated using T1 ρ imaging [15,16], sodium (^{23}Na) imaging [17,18], delayed gadolinium-enhanced MRI of cartilage (dGEMRIC) [19], or GAG chemical exchange saturation transfer (gagCEST) imaging [16,20].

Biochemical imaging by the gagCEST imaging could predict the depletion of GAGs in early OA, which is significant because evaluation of the concentration and distribution of GAGs is essential for the early diagnosis and potential treatment monitoring of OA [21,22]. Although the gagCEST imaging is usually applied using ultra-high field MR systems [23], a few clinical studies have demonstrated the feasibility of using the same with 3 T MR systems [24,25]. However, no study has hitherto evaluated the feasibility of gagCEST MRI in OA with the objective of demonstrating the association between the gagCEST sequence and pain scores. The purpose of this study was to assess the relationship between the magnetization transfer ratio asymmetry (MTR_{asym}) of gagCEST and pain scores according to the visual analog scale (VAS) in OA of the knee joint.

2. Materials and methods

2.1. Phantom preparation

A phantom study for the evaluation of the quantitative correlation between the MTR_{asym} values of gagCEST images and the concentration of GAGs was performed using hyaluronic acid. In order to simulate various concentrations of GAGs, phantoms consisting hyaluronic acid were prepared by dissolving the compound (molecular weight, 3 MDa; Dongkook Pharmaceutical Co. Ltd., Seoul, Korea) in deionized water. In order to minimize the effect of pH, the phantoms were titrated to pH 7.4 with 0.1 M solutions of hydrochloride and sodium hydroxide using a pH meter (F-74BW, Horiba Ltd., Kyoto, Japan). The phantoms, with GAG concentrations of 1.38, 2.75, 5.5, 11.0, and 22.0 mg/mL, were prepared in 1.7 mL microtubes. The phantoms were arranged in an agarose gel tray in order to achieve fixation and prevent the magnetic field inhomogeneity effect.

2.2. Phantom MRI protocol

Magnetic resonance imaging of the phantom with CEST was performed using a 3.0 T MR system (Achieva, Philips Healthcare,

Best, Netherlands) using an 8-channel phased-array wrist coil (Philips wrist coil, Philips Healthcare, Best, Netherlands) and a whole-body transmit coil. Ten images in the coronal plane were acquired using three-dimensional (3D) gradient-echo sequence with segmented echo-planar imaging (EPI) employing pulsed steady-state saturation [26]; saturation radiofrequency (RF) irradiation was performed prior to every EPI data readout, using a sinc-Gauss pulse with a peak amplitude of 3.5 μT and acquisition time of 70 ms, thus limiting the RF duty cycle to within 50% of that allowed by the MRI system. The other scanning parameters were as follows: repetition time (TR)/echo time (TE), 145.467/6.14 ms; slice thickness, 4 mm; slice overlap, 2 mm; FOV, 110 \times 110 \times 20 mm; acquisition matrix, 72 \times 66; flip angle, 7°; 55 offset frequencies ranging from -5 ppm to 5 ppm, at intervals of 24 Hz (0.19 ppm); and one reference scan.

2.3. Study population

The MR imagings of 22 patients (male, 9; female, 13) who underwent knee MRI including gagCEST imaging between September 2014 and December 2014 were retrospectively investigated. The mean age of the patients was 50.3 \pm 14.3 years (age range, 25–79 years). This study was reviewed and approved by the institutional review board.

2.4. Data of VAS pain scores from electronic medical records

The intensity of pain was evaluated using a 10-point VAS by trained orthopedic surgeons. The VAS pain scores, ranging from 0 to 10, within 2 weeks of MRI were recorded for each patient.

2.5. In vivo MRI protocol

Magnetic resonance imaging was performed using a 3.0 T MR system (Achieva, Philips Healthcare, Best, Netherlands) with a dedicated 8-channel SENSE knee coil (Invivo, Gainesville, FL, USA) and a whole-body transmit coil. The following imaging sequence for knee MRI was employed: a sagittal T2-weighted turbo spin echo (TSE) imaging with a repetition time (TR)/echo times (TE) of 2700/100 ms, a field of view (FOV) of 140 \times 140 mm, an acquisition matrix of 336 \times 263, and a slice thickness of 3 mm (interslice gap of 0.3 mm); an axial T1-weighted TSE with a TR/TE of 643/10 ms and an acquisition matrix of 360 \times 285; an axial T2-weighted TSE series with fat saturation, a TR/TE of 3080/62, and an acquisition matrix of 384 \times 297; a coronal T2-weighted TSE with fat saturation, a TR/TE of 2863/62 ms, and an acquisition matrix of 384 \times 306; and a sagittal 3D volume isotropic TSE acquisition (VISTA) imaging with fat suppression, a TR/TE of 1400/32 ms; 0.5 mm slice thickness and no interslice gap; FOV of 160 \times 160 mm, acquisition matrix of 320 \times 320, number of acquisitions of 1; and echo train length of 63.

Magnetic resonance imaging with CEST was performed using the 3D gradient-echo sequence in a protocol similar to that employed in the phantom study. Images were acquired at the PFJ level in the axial plane. Acquisition of the CEST-weighted images was performed using the following imaging parameters: TR/TE, 140/8.176 ms; slice thickness, 6 mm; slice overlap, 3 mm; FOV, 120 \times 120 \times 18 mm; acquisition matrix, 128 \times 120; flip angle, 7°; peak RF amplitude, 3.5 μT ; 59 offset frequencies ranging from -5 ppm to 5 ppm, at intervals of 22 Hz (0.17 ppm); and one reference scan (S0). The S0 scan was acquired with far offset RF frequency ($-100,000$ Hz), which was equivalent to the scan acquired without saturation RF, for normalization of CEST Z-spectral data and calculation of magnetization transfer ratio asymmetry. We used segmented steady-state approach by Sled and Pike [26], where 70 ms saturation RF was followed by segmented 3D gradient-echo EPI readout limited at 50%

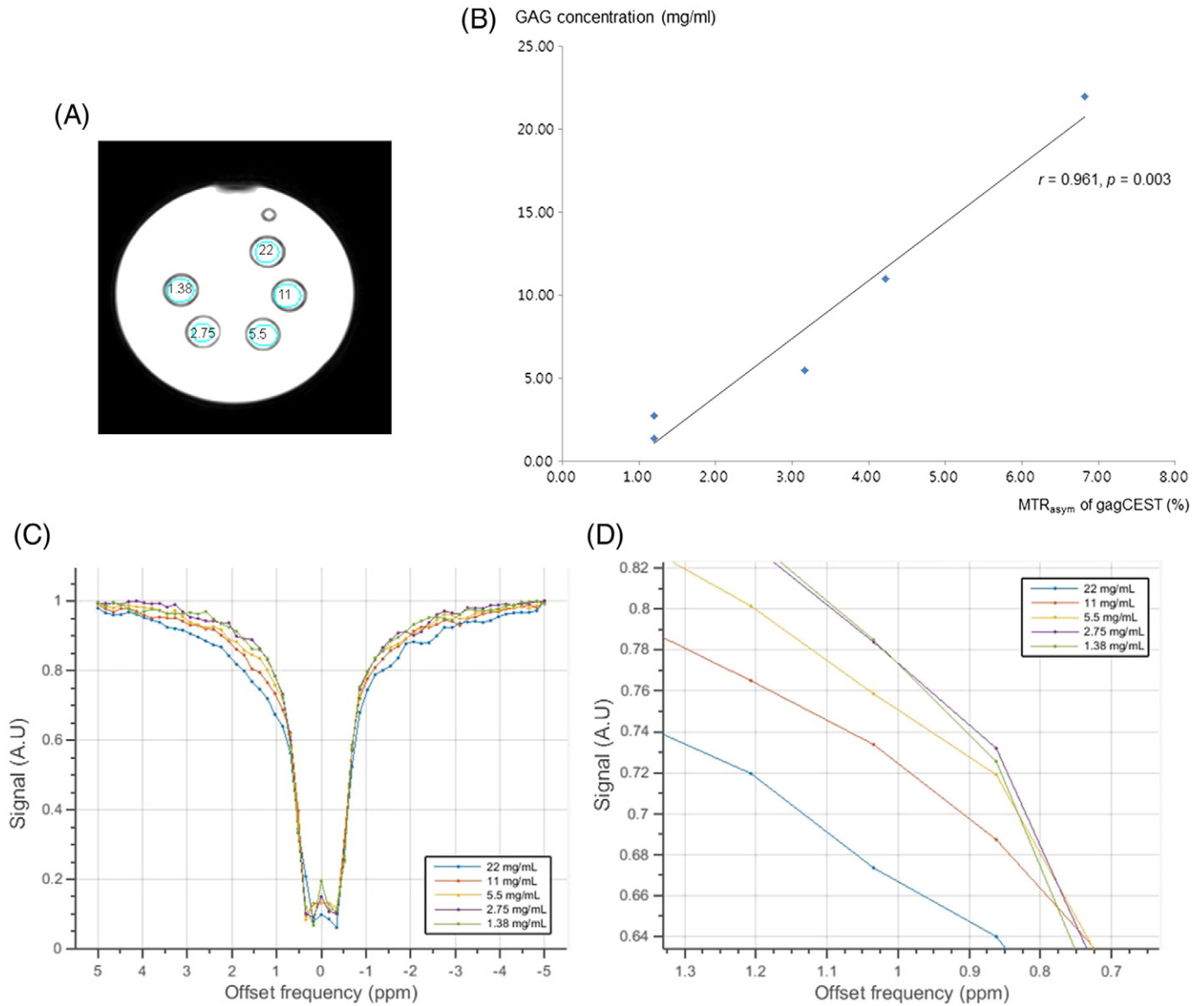


Fig. 1. Scatter plot of the concentrations of GAGs estimated using the MTR_{asym} of the gagCEST images in comparison with the concentrations of GAGs in the phantom. A. Phantom image of the five different concentrations (1.38, 2.75, 5.5, 11.0, and 22.0 mg/mL) of GAGs. B. Analysis of MTR_{asym} values of the gagCEST images revealed excellent correlation between MTR_{asym} values and concentration of GAGs. GAG, glycosaminoglycan; MTR_{asym} , magnetization transfer ratio asymmetry; gagCEST, glycosaminoglycan chemical exchange saturation transfer. C. ROI averaged Z-spectrum. Gag concentration-dependent CEST effect is presented at 1.0 ppm. D. Z-spectrum magnified around 1.0 ppm. It represent gag concentration-dependent CEST effects. Abbreviations: MTR_{asym} , magnetization transfer ratio asymmetry; GAG, glycosaminoglycan; gagCEST, GAG chemical exchange saturation transfer (gagCEST); CEST, chemical exchange saturation transfer.

RF duty cycle and clinically allowable SAR. The total scan time was 4 min 55 s for six slices.

2.6. Post-processing of MR images and analysis of MTR_{asym}

In order to calculate the MTR_{asym} values of the CEST MR images, all data were transferred to an offline personal computer for analysis using in-house software programmed by Interactive Data Language (IDL; Exelis VIS Inc., Boulder, CO, USA). All of the CEST MR images were analyzed by a board-certified musculoskeletal radiologist with 12 years of experience in random scanning, blinded to patient history. For each MR image, an elliptical region of interest (ROI; average number of pixels, 35–50) was placed over the cartilage on the patellar facet or femoral trochlea.

For gagCEST MR imaging, the CEST effect within each ROI was automatically determined as the absolute value at the offset of ± 1.0 ppm after correction of the B_0 field inhomogeneity effect. To account for the B_0 field inhomogeneity effect in CEST imaging, the Z-spectrum was fit to 12th order polynomial and then the fit was interpolated at 1 Hz resolution to determine the minimum signal for the identification of B_0 offset as performed in Zhou et al. [27]. The MTR_{asym} values of the gagCEST images were calculated according to the following equation:

$$MTR_{asym}(1.0\text{ ppm}) = MTR(+1.0\text{ ppm}) - MTR(-1.0\text{ ppm}) \\ = \frac{S_{sat}(-1.0\text{ ppm})}{S_0} - \frac{S_{sat}(+1.0\text{ ppm})}{S_0}$$

where, S_{sat} is the signal intensity when saturation RF pulses are applied at each frequency offset, and S_0 is the reference signal.

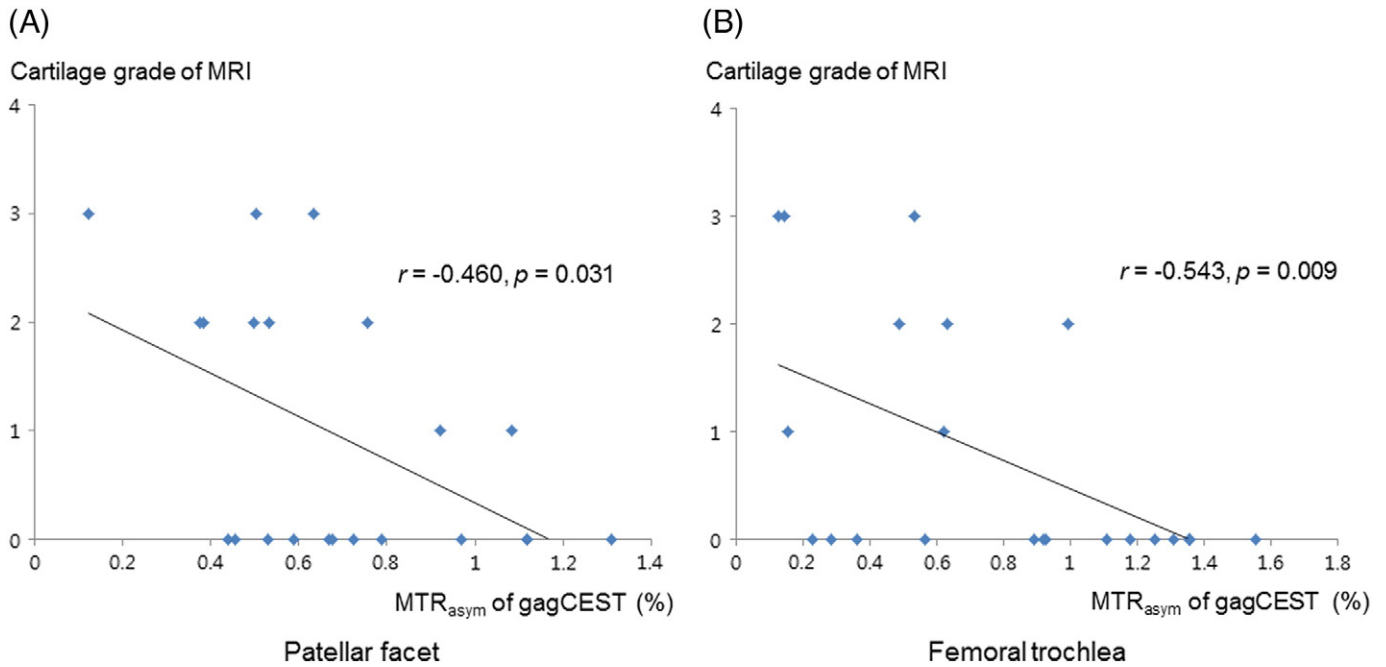


Fig. 2. Scatter plot of the correlation between the cartilage grades on MR images and the MTR_{asym} values of the gagCEST images. The patellar facet (A) as well as the femoral trochlea (B) show significant negative correlations between the two parameters. Abbreviations: MR, magnetic resonance; MTR_{asym}, magnetization transfer ratio asymmetry; gagCEST, glycosaminoglycan chemical exchange saturation transfer.

2.7. Qualitative analysis of cartilage grading

The radiologists who graded the cartilages were blinded to the arthroscopic findings and medical records of the patients. They graded the patellar facet and femoral trochlea of the PFJ visualized in the knee MR images, according to the Outerbridge classification system [28,29].

The cartilage grades were defined as follows: grade 0, intact cartilage; grade 1, signal change on T2-weighted MR images; grade 2, cartilage defect less than 50% of the depth; grade 3, cartilage defect more than 50% of the depth; and grade 4, full-thickness cartilage defect along with exposure of the subchondral bone. When multiple cartilaginous lesions were present, the lesion with the highest grade was recorded.

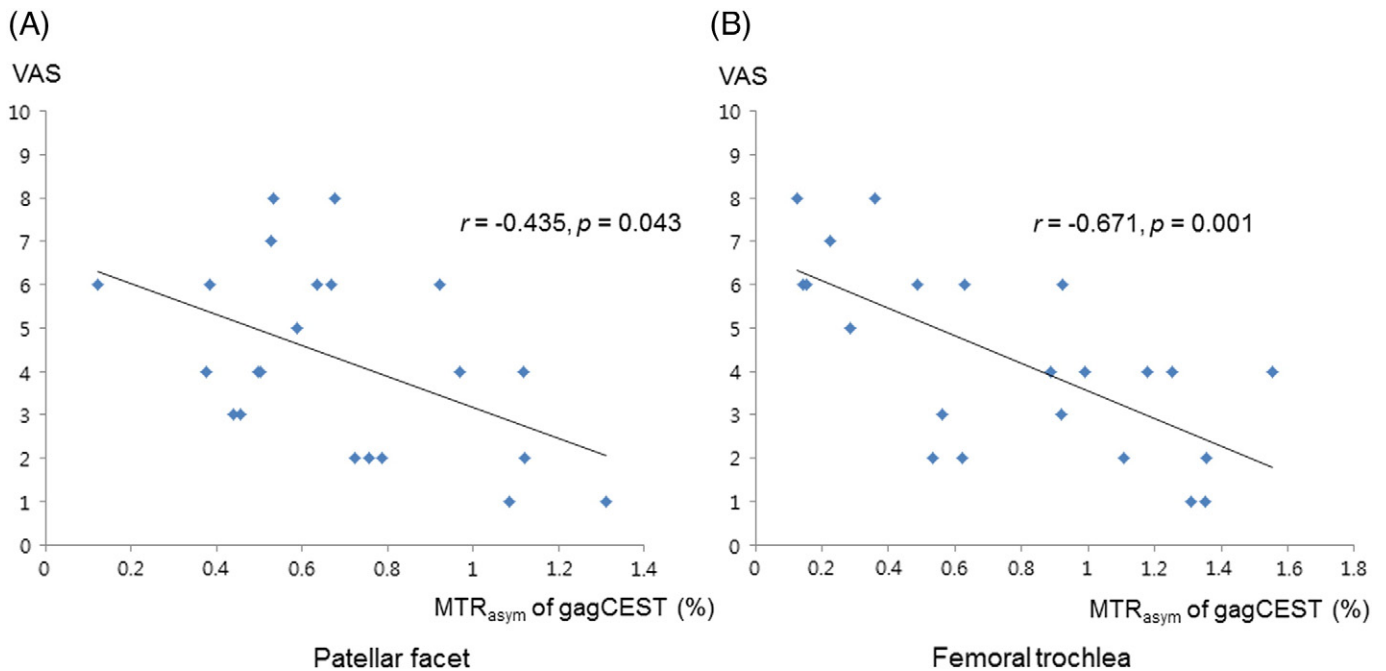


Fig. 3. Scatter plot of the correlation between the VAS pain scores and the MTR_{asym} values of the gagCEST images. The patellar facet (A) as well as femoral trochlea (B) show significant negative correlations between the two parameters. Abbreviations: VAS, visual analog scale; MTR_{asym}, magnetization transfer ratio asymmetry; gagCEST, glycosaminoglycan chemical exchange saturation transfer.

Table 1

Spearman's correlation coefficients between the VAS pain scores and the MTR_{asym} values and cartilage grades of the patellar facet and femoral trochlea.

	Patellar facet		Femoral trochlea	
	Cartilage grade	VAS score	Cartilage grade	VAS score
MTR_{asym} (%)	-0.460 (0.031)*	-0.435 (0.043)*	-0.543 (0.009)**	-0.671 (0.001)**

The data are presented as the Spearman's correlation coefficient (p value).

Abbreviations: MTR_{asym} , magnetization transfer ratio asymmetry; VAS, visual analog scale.

* Significant correlation at $p < 0.05$.

** Significant correlation at $p < 0.01$.

2.8. Statistical analysis

Intraobserver agreements for agarose phantom were evaluated with the intraclass correlation coefficient (ICC). The correlations of the VAS pain scores with the cartilage grades according to the MRI findings and the MTR_{asym} values of the patellar and trochlear cartilage were assessed using the Spearman's correlation coefficients. All statistical analyses were performed in the R programming environment (R package version 3.1.2, R Foundation of Statistical Imaging, Vienna, Austria; <http://cran.r-project.org>). Values of $p < 0.05$ were considered statistically significant.

3. Results

In the phantom study, the MTR_{asym} values of gagCEST images showed excellent correlation with the concentration of GAGs ($r = 0.961$; $p = 0.003$; Fig. 1). Intraobserver agreements for the agarose phantom showed excellent correlation (ICC = 0.987). The MTR_{asym} was observed to increase with the increase in the concentration of GAGs.

In the study population, the cartilage grades according to the MR images were significantly and negatively correlated with the MTR_{asym} values in the patellar facet as well as the femoral trochlea ($r = -0.460$, $p = 0.031$ and $r = -0.543$, $p = 0.009$, respectively; Fig. 2A and 2B).

The knee pain scores measured according to the VAS were significantly and negatively correlated with the MTR_{asym} values in the patellar facet as well as the femoral trochlea ($r = -0.435$, $p = 0.043$

and $r = -0.671$, $p = 0.001$, respectively; Fig. 3A and B). The results of correlation analysis are summarized in Table 1.

The MTR_{asym} maps revealed high concentrations of GAGs in patients with low grades of cartilage and low pain scores (Fig. 4). Additionally, they revealed low concentrations of GAGs in patients with high grades of cartilage and high pain scores (Fig. 5). However, this inverse correlation was not observed in some of the patients evaluated in the present study (Fig. 6).

4. Discussion

The knee joint is a tri-compartmental joint and includes the PFJ as well as the medial and lateral TFJ. The PFJ is an important source of the symptoms associated with knee OA, possibly more important than the TFJ. Despite its high prevalence, relatively little research has been directed toward patellofemoral OA. The relationship between the radiographic features of patellofemoral OA and knee pain has been reported as has the relationship between knee symptoms and cartilage volume according to MRI findings [7,30,31]. Reduced patellar cartilage volume, measured on MR images, has been reported to be associated with knee pain [32]. In the present study, we have demonstrated that the MTR_{asym} values of gagCEST imaging as well as the cartilage grades according to the MRI findings exhibit changes proportional to the patient pain scores measured according to the VAS, which is consistent with the results of a previous study [32]. Furthermore, in the present study, the MTR_{asym} values of gagCEST imaging exhibited greater correlation with the pain scores than the morphological changes observed on conventional MR images.

Patellofemoral OA occurs when the articular cartilages of the femoral trochlea and patella facets become worn and inflamed. Early diagnosis and prompt treatment of this condition requires imaging of cartilage loss. Histologically, the cartilage is composed of approximately 70–80% water and 20–30% solid extracellular matrix (ECM) [33]. The main components of the ECM are collagen and proteoglycan molecules. Proteoglycans are heavily glycosylated protein monomers, and they represent the second largest group of macromolecules in the ECM of articular cartilages, accounting for 10–15% of the wet weight. They consist of a protein core with one or more covalently attached linear glycosaminoglycan (GAG) chains [33–35]. Therefore, quantitative evaluation of GAGs, which serve as biomarkers for OA, plays an important role in the diagnosis of the condition.

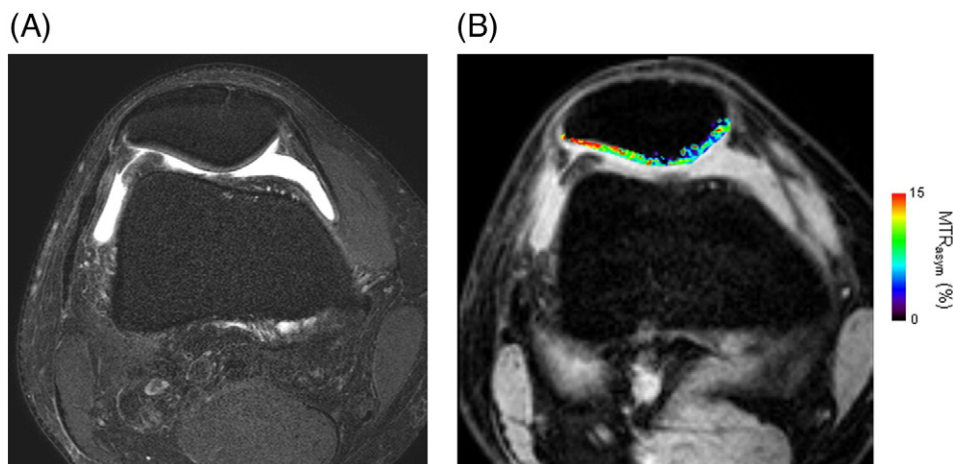


Fig. 4. A 36-year-old man with a knee pain score of 4. (A) Fat-saturated T2-weighted image shows cartilage of grade 0, without any signal change. (B) The MTR_{asym} map shows high concentrations of GAGs. The ROIs at the patellar facet show an MTR_{asym} value of 1.118%. Abbreviations: MTR_{asym} , magnetization transfer ratio asymmetry; GAG, glycosaminoglycan; ROI, region of interest.

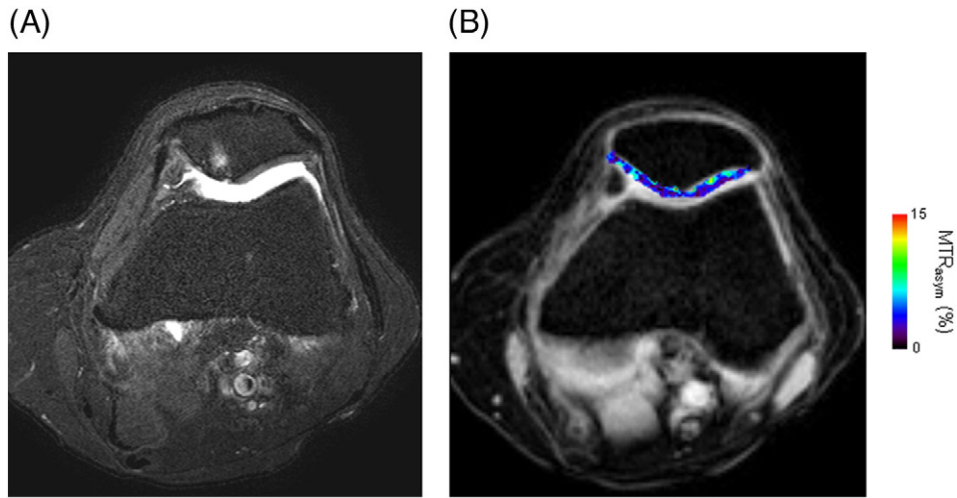


Fig. 5. A 74-year-old woman with a knee pain score of 6. (A) Fat-saturated T2-weighted image shows cartilage of grade 3, with high signal intensity and cartilage defects. (B) The MTR_{asymp} map shows decreased concentrations of GAGs. The ROIs at the patellar facet show an MTR_{asymp} value of 0.634%. Abbreviations: MTR_{asymp} , magnetization transfer ratio asymmetry; GAG, glycosaminoglycan; ROI, region of interest.

The hydroxyl groups in GAGs can be visualized quantitatively using the magnetization transfer imaging technique, in which, off-resonance RF saturation pulses are applied at frequencies specific to chemically exchangeable protons residing on the hydroxyl groups of cartilaginous GAGs [23]. As previously stated, imaging of GAGs can be performed using the T1 ρ , gagCEST, and ^{23}Na imaging techniques as well as dGEMRIC. Unlike dGEMRIC, the gagCEST method does not require the administration of a contrast agent. In addition, ^{23}Na imaging has the drawbacks of extremely low signal-to-noise ratio and relatively short transverse relaxation times, thus requiring ^{23}Na -tuned RF coils and optimization for faster imaging acquisition.

The chemical exchange-dependent saturation transfer technique can detect endogenous macromolecules indirectly through proton exchange with free water protons [20,23]. This imaging technique can be applied for the non-invasive monitoring of changes in knee cartilage in terms of the concentration of GAGs. It is considered a feasible method for imaging GAGs and overcoming the practical limitations of dGEMRIC and ^{23}Na imaging. Although, based on initial reports, the gagCEST method was believed to require ultra-high field

MR systems, recent cartilage studies using the gagCEST method have reported the technique to be feasible with 3 T MR systems [23–25]. *In vivo* feasibility studies using gagCEST MRI have shown the technique to be sensitive to GAG levels in cartilage [23]. In our phantom study, the MTR_{asymp} values of the gagCEST images also showed excellent correlation with the concentration of GAGs. In general, the cartilage grades according to the MRI findings and the MTR_{asymp} values of the gagCEST images were found to be inversely correlated (Figs. 4 and 5). Moreover, the VAS pain scores were also inversely correlated with the MTR_{asymp} values. As shown in Fig. 6, a patient with a low grade of cartilage according to MRI findings and low concentration of GAGs exhibited significantly high pain scores, suggesting that the knee pain more likely resulted from low GAG concentrations rather than gross cartilaginous defects.

The strength of the present study is the evaluation of the relationship between the symptoms of OA of the knee and the MTR_{asymp} values of gagCEST imaging. The correlation between symptoms of OA of the knee and MTR_{asymp} could help understand the mechanism of pain and address the treatment guidelines. In the

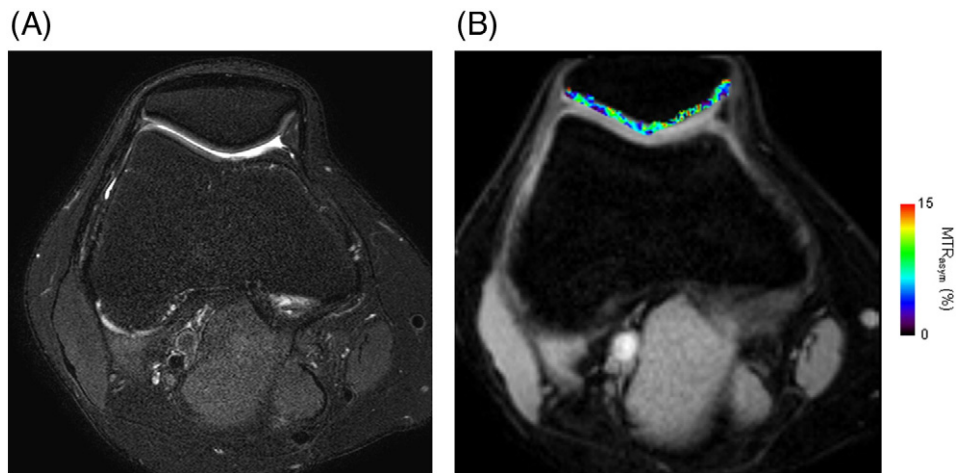


Fig. 6. A 31-year-old man with a knee pain score of 6. (A) Fat-saturated T2-weighted image shows cartilage of grade 0, with no signal change or gross cartilage defects. (B) The MTR_{asymp} map shows decreased concentrations of GAG. The ROIs at the patellar facet show an MTR_{asymp} value of 0.667%. The VAS pain score is 6. This case shows low concentrations of GAG on MTR_{asymp} although conventional fat-saturated T2-weighted image shows no signal change or gross cartilage defects. Abbreviations: MTR_{asymp} , magnetization transfer ratio asymmetry; GAG, glycosaminoglycan; ROI, region of interest; VAS, visual analog scale.

present study, the correlation observed between the quantitative MR imaging findings and gagCEST imaging findings of knee pain might serve not only as a biomarker, but also as a new approach for the evaluation of OA treatment in terms of monitoring treatment outcome.

The results of a technical comparison study of gagCEST with dGEMRIC and T2 imaging revealed that gagCEST exhibited similar efficacy as the other two protocols in distinguishing healthy cartilage from the damaged one [25] and suggested the clinical feasibility of using the gagCEST protocol with 3 T MR systems. The results of our study showed good correlation of the MTR_{asym} values of the gagCEST images and the concentrations of GAGs, which is in concordance with the results of previous studies on the evaluation of GAG concentrations [23,24,36]. However, in the preset study, we were unable to compare efficacy of the gagCEST protocol with that of the T1 ρ protocol because of limitations in MR image acquisition. Further studies are necessary in order to establish the potential value of gagCEST in the assessment of OA-related cartilage degeneration.

There are a few technical issues pertaining to gagCEST. First, the range of off-resonance RF saturation pulses should be optimized for gagCEST imaging protocols. We validated the correlation of MTR_{asym} values of the gagCEST images with the concentration of GAGs based on the results of the phantom study. We also optimized the following image acquisition parameters for gagCEST through the phantom study – peak amplitude of 3.5 μ T and 60 offset frequencies ranging from –5 ppm to 5 ppm. We believe that optimization of the gagCEST imaging protocol can be achieved by focusing on off-resonance RF saturation pulses around 1 ppm and –1 ppm instead of the entire range. Second, the z-spectrum fitting model for gagCEST imaging has yet to be determined. Finally, we expect that more accurate CEST effect might be evaluated with use of WASSR scan because gagCEST values were more reliable using a low saturation B1 WASSR scan [37].

The present study had several limitations. First, since this study was retrospective in nature, we were unable to compare the changes in the follow-up values of MTR_{asym} of the gagCEST images between the symptoms of OA of the knee and the T2 values. Second, the MR images were acquired with the knees flexed at approximately 10–15 degree angles within dedicated quadrature knee coils. Consequently, the patellofemoral measurements might have been influenced by the position of the knee during imaging. In order to minimize the variation because of knee positioning during imaging, we carefully checked the position of the knee in the knee coil during imaging. In order to minimize the interobserver and intraobserver variations of the values of MTR_{asym} of the gagCEST images, the mean values of repeat measurements of the MTR_{asym} of the gagCEST images were used for analysis. Finally our study was performed at 3 T MRI imager. A previous comparison study of 3 T and 7 T showed gagCEST of 3 T was less useful than that of 7 T [38] although some reports showed the feasibility at a 3 T [23–25]. Besides the low sensitivity at 3 T, we think that the tendency of pain and GAG concentration could be demonstrated at our study using 3 T MR imager. We expect that this kind of the clinical pain correlation study of gagCEST will be performed at 7 T MR imager.

In conclusion, the cartilage grade of MR images and knee pain scores was significantly and negatively correlated with MTR_{asym} . The biochemical changes, visualized in terms of MTR_{asym} values of the gagCEST images, exhibited greater correlation with the pain scores than the morphological changes visualized on conventional MR images. These results provide evidence supporting the theory regarding the association of patellofemoral OA and knee pain scores.

References

- [1] Hill CL, Hunter DJ, Niu J, Clancy M, Guermazi A, Genant H, et al. Synovitis detected on magnetic resonance imaging and its relation to pain and cartilage loss in knee osteoarthritis. *Ann Rheum Dis* 2007;66(12):1599–603.
- [2] Ayrar X, Ravaut P, Bonvarlet JP, Simonnet J, Lecurieux R, Nguyen M, et al. Arthroscopic evaluation of post-traumatic patellofemoral chondropathy. *J Rheumatol* 1999;26(5):1140–7.
- [3] Hinman RS, Crossley KM. Patellofemoral joint osteoarthritis: an important subgroup of knee osteoarthritis. *Rheumatology (Oxford)* 2007;46(7):1057–62.
- [4] Kim YM, Joo YB. Patellofemoral osteoarthritis. *Knee Surg Relat Res* 2012;24(4):193–200.
- [5] Iwano T, Kurosawa H, Tokuyama H, Hoshikawa Y. Roentgenographic and clinical findings of patellofemoral osteoarthritis. With special reference to its relationship to femorotibial osteoarthritis and etiologic factors. *Clin Orthop Relat Res* 1990;252:190–7.
- [6] Besier TF, Pal S, Draper CE, Fredericson M, Gold GE, Delp SL, et al. The role of cartilage stress in patellofemoral pain. *Med Sci Sports Exerc* 2015;47(11):2416–22.
- [7] Ruiz Santiago F, Pozuelo Calvo R, Almansa Lopez J, Guzman Alvarez L, Castellano Garcia Mdel M. T2 mapping in patellar chondromalacia. *Eur J Radiol* 2014;83(6):984–8.
- [8] Koff MF, Amrami KK, Kaufman KR. Clinical evaluation of T2 values of patellar cartilage in patients with osteoarthritis. *Osteoarthritis Cartilage* 2007;15(2):198–204.
- [9] Menezes NM, Gray ML, Hartke JR, Burstein D. T2 and T1rho MRI in articular cartilage systems. *Magn Reson Med* 2004;51(3):503–9.
- [10] Toffanin R, Mlynarik V, Russo S, Szomolanyi P, Piras A, Vittur F. Proteoglycan depletion and magnetic resonance parameters of articular cartilage. *Arch Biochem Biophys* 2001;390(2):235–42.
- [11] Subhawong TK, Thakkar RS, Padua A, Flammang A, Chhabra A, Carrino JA. Patellofemoral friction syndrome: magnetic resonance imaging correlation of morphologic and T2 cartilage imaging. *J Comput Assist Tomogr* 2014;38(2):308–12.
- [12] Bining HJ, Santos R, Andrews G, Forster BB. Can T2 relaxation values and color maps be used to detect chondral damage utilizing subchondral bone marrow edema as a marker? *Skeletal Radiol* 2009;38(5):459–65.
- [13] Dunn TC, Lu Y, Jin H, Ries MD, Majumdar S. T2 relaxation time of cartilage at MR imaging: comparison with severity of knee osteoarthritis. *Radiology* 2004;232(2):592–8.
- [14] Welsch GH, Mamisch TC, Domayer SE, Dorotka R, Kutscha-Lissberg F, Marlovits S, et al. Cartilage T2 assessment at 3-T MR imaging: *in vivo* differentiation of normal hyaline cartilage from reparative tissue after two cartilage repair procedures – initial experience. *Radiology* 2008;247(1):154–61.
- [15] Prasad AP, Nardo L, Schooler J, Joseph GB, Link TM. T(1)rho and T(2) relaxation times predict progression of knee osteoarthritis. *Osteoarthritis Cartilage* 2013;21(1):69–76.
- [16] Yao W, Qu N, Lu Z, Yang S. The application of T1 and T2 relaxation time and magnetization transfer ratios to the early diagnosis of patellar cartilage osteoarthritis. *Skeletal Radiol* 2009;38(11):1055–62.
- [17] Madelin G, Regatte RR. Biomedical applications of sodium MRI *in vivo*. *J Magn Reson Imaging* 2013;38(3):511–29.
- [18] Wheaton AJ, Borthakur A, Shapiro EM, Regatte RR, Akella SV, Kneeland JB, et al. Proteoglycan loss in human knee cartilage: quantitation with sodium MR imaging – feasibility study. *Radiology* 2004;231(3):900–5.
- [19] Burstein D, Velyvis J, Scott KT, Stock KW, Kim YJ, Jaramillo D, et al. Protocol issues for delayed Gd(DTPA)(2-)–enhanced MRI (dGEMRIC) for clinical evaluation of articular cartilage. *Magn Reson Med* 2001;45(1):36–41.
- [20] Regatte RR, Akella SV, Reddy R. Depth-dependent proton magnetization transfer in articular cartilage. *J Magn Reson Imaging* 2005;22(2):318–23.
- [21] Akella SV, Regatte RR, Gougoutas AJ, Borthakur A, Shapiro EM, Kneeland JB, et al. Proteoglycan-induced changes in T1rho-relaxation of articular cartilage at 4 T. *Magn Reson Med* 2001;46(3):419–23.
- [22] Tratten S, Marlovits S, Gebetsroither S, Szomolanyi P, Welsch GH, Salomonowitz E, et al. Three-dimensional delayed gadolinium-enhanced MRI of cartilage (dGEMRIC) for *in vivo* evaluation of reparative cartilage after matrix-associated autologous chondrocyte transplantation at 3.0 T: preliminary results. *J Magn Reson Imaging* 2007;26(4):974–82.
- [23] Ling W, Regatte RR, Navon G, Jerschow A. Assessment of glycosaminoglycan concentration *in vivo* by chemical exchange-dependent saturation transfer (gagCEST). *Proc Natl Acad Sci U S A* 2008;105(7):2266–70.
- [24] Schleich C, Bittersohl B, Miese F, Schmitt B, Muller-Lutz A, Sondern M, et al. Glycosaminoglycan chemical exchange saturation transfer at 3 T MRI in asymptomatic knee joints. *Acta Radiol* 2015.
- [25] Rehnitz C, Kupfer J, Streich NA, Burkholder I, Schmitt B, Lauer L, et al. Comparison of biochemical cartilage imaging techniques at 3 T MRI. *Osteoarthritis Cartilage* 2014;22(10):1732–42.
- [26] Sled JG, Pike GB. Quantitative imaging of magnetization transfer exchange and relaxation properties *in vivo* using MRI. *Magn Reson Med* 2001;46(5):923–31.
- [27] Zhou J, Zhu H, Lim M, Blair L, Quinones-Hinojosa A, Messina SA, et al. Three-dimensional amide proton transfer MR imaging of gliomas: initial experience and comparison with gadolinium enhancement. *J Magn Reson Imaging* 2013;38(5):1119–28.
- [28] Potter HG, Linklater JM, Allen AA, Hannafin JA, Haas SB. Magnetic resonance imaging of articular cartilage in the knee. An evaluation with use of fast-spin-echo imaging. *J Bone Joint Surg Am* 1998;80(9):1276–84.
- [29] Suh JS, Lee SH, Jeong EK, Kim DJ. Magnetic resonance imaging of articular cartilage. *Eur Radiol* 2001;11(10):2015–25.
- [30] Dowd GS, Bentley G. Radiographic assessment in patellar instability and chondromalacia patellae. *J Bone Joint Surg (Br)* 1986;68(2):297–300.

- [31] Insall J, Falvo KA, Wise DW. Chondromalacia patellae. A prospective study. *J Bone Joint Surg Am* 1976;58(1):1–8.
- [32] Hunter DJ, March L, Sambrook PN. The association of cartilage volume with knee pain. *Osteoarthritis Cartilage* 2003;11(10):725–9.
- [33] Binks DA, Hodgson RJ, Ries ME, Foster RJ, Smye SW, McGonagle D, et al. Quantitative parametric MRI of articular cartilage: a review of progress and open challenges. *Br J Radiol* 2013;86(1023):20120163.
- [34] Buckwalter JA, Mankin HJ. Articular cartilage: degeneration and osteoarthritis, repair, regeneration, and transplantation. *Instr Course Lect* 1998;47:487–504.
- [35] Sophia Fox AJ, Bedi A, Rodeo SA. The basic science of articular cartilage: structure, composition, and function. *Sports Health* 2009;1(6):461–8.
- [36] Lee JS, Parasoglou P, Xia D, Jerschow A, Regatte RR. Uniform magnetization transfer in chemical exchange saturation transfer magnetic resonance imaging. *Sci Rep* 2013;3:1707.
- [37] Krishnamoorthy G, Nanga RP, Bagga P, Hariharan H, Reddy R. High quality three-dimensional gagCEST imaging of *in vivo* human knee cartilage at 7 Tesla. *Magn Reson Med* 2016.
- [38] Singh A, Haris M, Cai K, Kassey VB, Kogan F, Reddy D, et al. Chemical exchange saturation transfer magnetic resonance imaging of human knee cartilage at 3 T and 7 T. *Magn Reson Med* 2012;68(2):588–94.